2015 IEEE International Conference on Advanced Intelligent Mechatronics (AIM)
July 7-11, 2015. Busan, Korea

Vision-Based Path Coordination for Multiple Mobile Robots with Four Steering Wheels Using an Overhead Camera

Zahra Ziaei, Reza Oftadeh, Jouni Mattila*

***Abstract*— In this paper, we extend our previous work to introduce a vision-based path coordination method for multiple mobile robots with four steering wheels to avoid mutual collisions, so that the generated paths are always in the visibility range of the overhead camera. The proposed algorithm generates the synchronized trajectories for all wheels belonging to each mobile robot, with respect to its inertial-frame, relying on only one calibrated camera. These synchronized trajectories reduce the complexity of the robot kinematic model to plan maximum allowable bounded driving and steering velocities for each mobile robot. The main contribution of the proposed method is coordinating the trajectories for multiple mobile robots to avoid intersection boundaries that are obtained by generated geometrical traces in real world coordinates. Our experimental results are presented to illustrate the efficiency of the proposed method for the path coordination of multiple mobile robots with four steering wheels to avoid mutual collision.**

***Index Terms*— Path coordination, Multiple mobile robots, Vision-based method, Four steering wheels, Nonholonomic mobile robots, Steering and driving velocity, Intersection region.**

I. Introduction

Multiple mobile robots have been widely used in industrial and scientific applications to accomplish tasks, such as transportation, inspection and manipulation, in environments that are inaccessible to humans [1]. The coordination of the motion of mobile robots in a shared workspace, so that they avoid collision, is known as the multiple mobile robot path coordination problem [2], [3].

In this paper, we address the problem of coordinating the multiple mobile robots with four-wheel-steered (4WS) in the shared workspace. They must avoid mutual collisions, to reach their independent goals, so that the generated paths are always in the camera field of view, guaranteeing that the robots stay in the visibility range of the overhead camera. A mobile robot with 4WS is a type of nonholonomic mobile robot with omnidirectional steering wheels that are able to move along any direction, simultaneously attaining desired orientation [4], [5]. Such robots are more flexible than ordinary holonomic mobile robots which makes them suitable for confined work spaces, such as working in the camera field of view [6]. The main motivation of this work is to take advantage of the proposed method for inspection and manipulation tasks in confined and out-of-reach work spaces, such as the CERN[1] tunnel in which the main reliable feedback is a monocular vision-system. Multiple robots path coordination algorithms can be divided into two categories: centralized and decentralized algorithms [7], [8], [9]. A centralized planner computes a path and motion in the combined configuration space, which consider the robots as a single combined robot, necessarily. In a decoupled approach, separate paths for each robot are computed independently, then a coordination diagram plans mutual collision-free trajectories for each robot along its path. Decoupled path coordination produce the results more faster than centralize method, but its quality is not guaranteed [8].

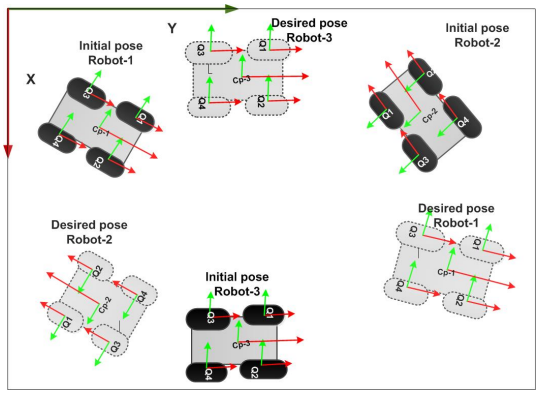

Fig. 1. Multiple mobile robots with four steering wheels move from initial to desired configurations in their shared workspace.

During the past decade, various path and trajectory planning methods for single mobile robots in relatively static environments have been presented [10], [11]. Additionally, several path and trajectory coordination methods have been proposed for multiple mobile robots in a shared workspace [2], [3], [12]. However, the major drawback of these methods is their relative complexity in the kinematic and dynamic models, and the need to design separate controllers for each robots position and orientation [13]. The most distinguishing aspect of multiple mobile robots, compared with a single mobile robot, is the possibility of mutual collision. Since an intersection test between mutual mobile robots can be expensive, swept volume computation [14] that determines the geometrical intersection boundaries to avoid mutual collision is a key solution. In this paper, we extend our previous work in path planning [15], to present the decoupled path coordination method based on a vision system that provides the necessary information about obstacles as well as the mobile robot's position and orientation in the initial and desired poses. Then, the synchronized trajectories for each mobile robot's wheels and center-frame are generated simultaneously. These synchronized trajectories simplify the

*Authors are with the Department of Intelligent Hydraulics and Automation (IHA), Tampere University of Technology, Tampere, Finland. zahra.ziaei@tut.fi, reza.oftadeh@tut.fi, jouni.mattila@tut.fi

[1]The European Organization for Nuclear Research

complexity of kinematic model for this type of mobile robots, significantly. Thus, we can compute the geometrical traces for actual volume of mobile robots and their possible intersection region, even in a confined shared workspace. Then, we plan the maximum allowable velocities for lower priority robots, taking into account the halting time to pass the intersection region by higher priority robot. We can continue this process for all mobile robots to reach their goals in the shared workspace.

The paper is organized as follows. In Section II, we review the vision-based path planning method for a single mobile robot. The proposed method simplifies the kinematic model of the mobile robot, which is described in Section III. Planning the bounded steering and driving velocity are addressed in Section IV. In Section V, the path coordination for multiple mobile robots with 4WS is explained. Depending on the size of the robots' platforms, limited number of mobile robot can move in the shared workspace. In Section VI, we show the efficiency of the proposed method for two and three mobile robots to reach their goals while avoiding static obstacles as well as mutual collision.

II. VISION-BASED PATH PLANNING FOR A SINGLE MOBILE ROBOT WITH 4WS

In this section, we review the vision-based path planning for a single mobile robot with 4WS, which was introduced in a previous paper [15]. This method defines the relationship between the motion of a mobile robot with 4WS in the image space and its corresponding motion in the world coordinates using an artificial potential field (APF) and visual servoing concepts. Figure 2 represents the system architecture that indicates the levels of the proposed method. The images that have already been grabbed in the initial and desired state of the mobile robot are the input data. Unlike the majority of conventional trajectory planning methods that consider the mobile robot as only one point, we consider the whole volume of the mobile robot as the four wheels' center-points plus the robot's center-point (robot-CP) that have the same rotations and different positions (Fig. 3).

Various methods exist for pose estimation of the desired points belonging to the mobile robot platform in the initial and desired states. We employ the CAD-based method [16], [17], to estimate the different positions and same orientation of the desired points $\mathbf{s} = \{Q_0, Q_1, ..., Q_4\}$ belonging to each robot (Fig. 3). To detect the static obstacle in the image according to its color, we employ the Hue-Saturation-Value (HSV) color filter to specify the boundaries of the obstacle in the image space. The obstacle-free path planning method presented in [15], proposed an artificial potential force in the image space to push the desired points of the platform away from the obstacles and pull them to reach the goal, simultaneously. This method presents the relationship between the generated trajectories in the image space and those corresponding in the 3D Cartesian workspace.

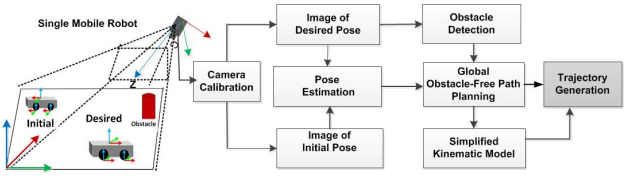

Fig. 2. System architecture of vision-based path planning for single mobile robot with 4WS [15].

A. Artificial Potential Fields and Forces

APF provides simple and efficient motion planners for practical purposes. The major problem in real-time path planning method using APF is the local-minimum issue, which can create a trap for the robot before it reaches its goal location. However, in an offline system (by considering the entire path), the problem of local minimum traps is greatly reduced, thereby allowing the method to be used for path planning [18]. Nonetheless, simple solutions have been proposed to avoid the local-minimum [19].

Here, the influence of the APF V in the image space is the sum of the following two terms. First is the attractive potential field V_{at}, whose role is to pull the robot's desired points toward the goal configuration parameterization workspace denoted by $\boldsymbol{\Upsilon}$. Second is the repulsive potential field V_{rp}, whose role is to push the robot's desired points away from constraints such as obstacles. At each iteration, our defined artificial potential force $F(\boldsymbol{\Upsilon})$ is induced by the potential function $F(\boldsymbol{\Upsilon}) = -\vec{\nabla}V$ where $\vec{\nabla}V$ denotes the gradient vector of V at the 6×1 vector $\boldsymbol{\Upsilon}$. It represents our desired parametetrization of the robot's workspace including the position and orientation of desired points belonging to the mobile robot. $F(\boldsymbol{\Upsilon}) = -\vec{\nabla}V$ where $\vec{\nabla}V$ can be decomposed as the sum of two vectors, $F_{at}(\boldsymbol{\Upsilon}) = -\vec{\nabla}V_{at}$ and $F_{rp}(\boldsymbol{\Upsilon}) = -\vec{\nabla}V_{rp}$ which are called the attractive and repulsive forces, respectively. The attractive potential field V_{at} is a parabolic function pulling the robot's desired points to the goal configuration simultaneously, to minimize the distance between the current poses and the desired poses in the 3D Cartesian workspace. We set $\boldsymbol{\Upsilon}_d = \mathbf{0}_{6\times1}$ as the desired destination of the robot's workspace and $V_{at} = \frac{1}{2}\alpha \| \boldsymbol{\Upsilon} - \boldsymbol{\Upsilon}_d \|^2$ or $V_{at} = \frac{1}{2}\alpha \| \boldsymbol{\Upsilon} \|^2$ where α is a positive scaling factor. Therefore, the attractive potential force is $\mathbf{F}_{at}(\boldsymbol{\Upsilon}) = -\vec{\nabla}V_{at} = -\alpha\boldsymbol{\Upsilon}$. The goal of the repulsive potential force is to push the robot's desired points away

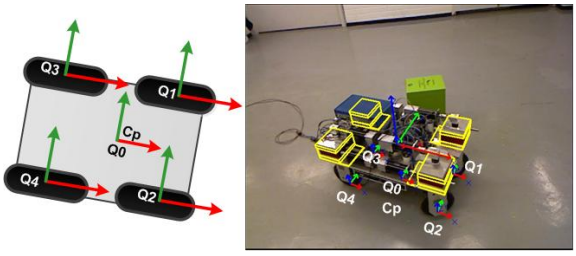

Fig. 3. Single mobile robot with 4WS and the recognized desired points include robot-CP denoted Q_0 and four wheels' center points denoted $\{Q_j, j = 1..., 4\}$ which mapped on the ground.

from the obstacles. Here, the desired repulsive potential force $\mathbf{F}_{rp}(\boldsymbol{\Upsilon}) = -\vec{\nabla} V_{rp}$ is the sum of two terms: the obstacle-avoidance-potential force in the image space $\mathbf{F}_{rp\mathcal{V}}(\boldsymbol{\Upsilon})$, and the visibility constraints of potential force $\mathbf{F}_{rp\mathcal{O}}(\boldsymbol{\Upsilon})$.

A visibility constraint implies a potential barrier force to push the mobile robot to reach the goal configuration while remaining in the camera's field of view. This force always keeps the generated path in the camera field of view guaranteeing that the robot stays in the visibility range of the overhead camera.

The total repulsive potential fields comprise the obstacle-avoidance and visibility constraint's repulsive potential fields. These potential field and force functions were introduced and presented in detail in our previous work [15].

$$\mathbf{F}_{rp}(\boldsymbol{\Upsilon}) = \mathbf{F}_{rp\mathcal{V}}(\boldsymbol{\Upsilon}) + \mathbf{F}_{rp\mathcal{O}}(\boldsymbol{\Upsilon}). \tag{1}$$

Total attractive and repulsive potential forces are:

$$\mathbf{F}(\boldsymbol{\Upsilon}) = \alpha \mathbf{F}_{at}(\boldsymbol{\Upsilon}) + \beta \mathbf{F}_{rp}(\boldsymbol{\Upsilon}), \tag{2}$$

where the attractive force denotes $\mathbf{F}_{at}(\Upsilon)$, the repulsive force denotes $\mathbf{F}_{rp}(\boldsymbol{\Upsilon})$, and $\boldsymbol{\Upsilon}$ is a 6×1 vector representing the parameterization of the robot's workspace induced by the proposed potential fields. Scale factors α and β are used to adjust the influence of the repulsive and attractive forces. The proposed mathematical potential functions for attractive and repulsive potential forces that define the relationship between the motion of the mobile robot in the image space and its corresponding motion in the 3D Cartesian workspace presented in [15].

B. Discrete-Time Trajectory

The discrete-time trajectory along the direction of $\boldsymbol{\Upsilon}$ is obtained by the transition equation which generates the midpoints from the initial to the robot's goal for all desired points belonging to the mobile robot, simultaneously [15]:

$$\boldsymbol{\Upsilon}_{k+1} = \boldsymbol{\Upsilon}_k + \epsilon_k \frac{\mathbf{F}(\boldsymbol{\Upsilon}_k)}{\| \mathbf{F}(\boldsymbol{\Upsilon}_k) \|}, \tag{3}$$

where k is an index that increases during the generation of a path, and $\epsilon_k$is a positive scaling factor. We allow the algorithm to generate sufficient number of midpoints by increasing ϵ_k. To turn the generated path into a trajectory, we must append a velocity component for each midpoint. The time values are chosen by spacing proportionally the distance between the two positions of the mobile robot-CP. Thus, the time between two consecutive mobile robot positions on the ground is constant: $\Delta t_k = t_k - t_{k-1}$. The distance between two successive positions $\boldsymbol{\Upsilon}_{\mathbf{k}}$ and $\boldsymbol{\Upsilon}_{\mathbf{k+1}}$ is chosen by fixing ϵ_k at a constant value via (3).

To minimize the distance between the current and desired poses in the 3D Cartesian workspace, we chose the parameterization workspace $\boldsymbol{\Upsilon}_c^T = [\mathbf{t}_c^T, (\mathbf{u}\theta)_{\mathbf{c}}^{\mathbf{T}}]$ with respect to the camera-frame, where u is the rotation axis, and θ is the rotation angle obtained from the rotation R between the initial and the desired poses with respect to the camera frame [15]. Thus, $\boldsymbol{\Upsilon}_i^T = [{}^{de}\mathbf{t}_{in}, {}^{de}(\mathbf{u}\theta)_i^T]$ and $\boldsymbol{\Upsilon}_{de}^T = 0_{6\times 1}$ show an initial and desired parametrization workspace. The homogeneous transformation matrices ${}^c\mathbf{T}_{in} = [{}^c\mathbf{R}_{in}, {}^c\mathbf{t}_{in}]$ and ${}^c\mathbf{T}_{de} = [{}^c\mathbf{R}_{de}, {}^c\mathbf{t}_{de}]$, where $\mathbf{t} \in \Re(3)$ and $\mathbf{R} \in SO(3)$, provide the rotation and translation of the vector of the desired points. The vector of the desired parameterization workspace $\boldsymbol{\Upsilon}$ is obtained via the following relation:

$$\begin{cases} {}^{de}\mathbf{R}_{in} = {}^{de}\mathbf{R}_c . {}^{in}\mathbf{R}_c^T \\ {}^{de}\mathbf{t}_{in} = -{}^{de}\mathbf{R}_{in} . {}^{in}\mathbf{t}_c + {}^{de}\mathbf{t}_c . \end{cases} \tag{4}$$

The visual servoing concepts in [15] define the relationship between the motion of the robot in the 2D image space to avoid a recognized obstacle and its corresponding motion in the 3D Cartesian workspace. Transformation of each k-th generated path to the camera center-frame is obtained via the following relations:

$$\begin{cases} {}^c\mathbf{R}_k = {}^k\mathbf{R}_{de}^T . {}^c\mathbf{R}_{de} \\ {}^c\mathbf{t}_k = {}^k\mathbf{R}_{de}^T ({}^c\mathbf{t}_{de} - {}^{de}\mathbf{t}_k). \end{cases} \tag{5}$$

The k-th generated trajectory with respect to the camera-frame in (5) for desired points $\{Q_i, i = 0...4\}$ is transformed to the mobile robot's inertial-frame Q, which has been previously estimated:

$$\begin{cases} {}^Q\mathbf{R}_k = {}^c\mathbf{R}_Q^T . {}^c\mathbf{R}_k \\ {}^Q\mathbf{t}_k = {}^c\mathbf{R}_Q^T . ({}^c\mathbf{t}_k - {}^c\mathbf{t}_Q). \end{cases} \tag{6}$$

Each generated k-th midpoint $[{}^Q\mathbf{t}_k, {}^Q\mathbf{R}_k]$ gives the position $(\hat{x_k}, \hat{y_k}, \hat{z_k})$ and the orientation $(\alpha_k, \beta_k, \theta_k)$ of the midpoints with respect to the robot's inertial-frame. However, the configuration of a mobile robot with 4WS is given by $(\hat{x_k}, \hat{y_k}, \theta_k)$, where $(\hat{x_k}, \hat{y_k})$ and θ_k represent the robot-CP and heading angle with respect to the inertial-frame, respectively.

III. KINEMATIC MODEL

Figure 4 illustrates the k-th generated midpoints of the synchronized trajectories for single mobile robot with 4WS in the world coordinates to show how can simplify the complexity of mobile robot kinematic model and obtain the kinematic variables. We assume the inertial-frame $\mathbf{U}\{\hat{\mathbf{X}}, \hat{\mathbf{Y}}\}$ is attached to the fixed robot-CP at the starting point Q. The heading frame $\mathbf{B}\{\hat{\mathbf{x_0}}, \hat{\mathbf{y_0}}\}$ coincides with the k-th generated trajectory point of robot-CP which is denoted by Q_0. The robot velocity frame $\mathbf{B}_v\{\hat{\mathbf{u}}, \hat{\mathbf{v}}\}$ is obtained using the tangent of the generated trajectory point in Q_0. Both frames $\mathbf{B}$ and $\mathbf{B}_v$ are attached to the robot's base at Q_0. The direction of the linear velocity vector in Q_0 is determined by the unit vector $\hat{\mathbf{v}}$ and its magnitude scalar v.

Using the k-th generated trajectories, we can obtain the rotation angle of mobile robot θ_B with respect to the inertial frame, Q, in the X direction. θ_B and ψ_v show the angles $\hat{\mathbf{x_0}}$ and $\hat{\mathbf{v}}$ in Q_0, respectively. Therefore, variables $\omega_B = \dot{\theta_B}$ and $\omega_v = \dot{\psi_v}$ are the angular velocities of the robot coordinates Q_0, and of $\hat{\mathbf{v}}$ and $\hat{\mathbf{x_0}}$ respectively.

The constant vectors $\overrightarrow{Q_0 Q_j}$ presented in frame $\mathbf{B}$ are denoted by $\{{}^{\mathbf{B}}\ell_{\mathbf{j}}, j = 1..., 4\}$. Angles $\{\phi_j, j = 1..., 4\}$ are the steering angles of the j-th wheel. Therefore, ${}^{\mathbf{B}}\hat{\mathbf{v}}_{\mathbf{j}}$ can be

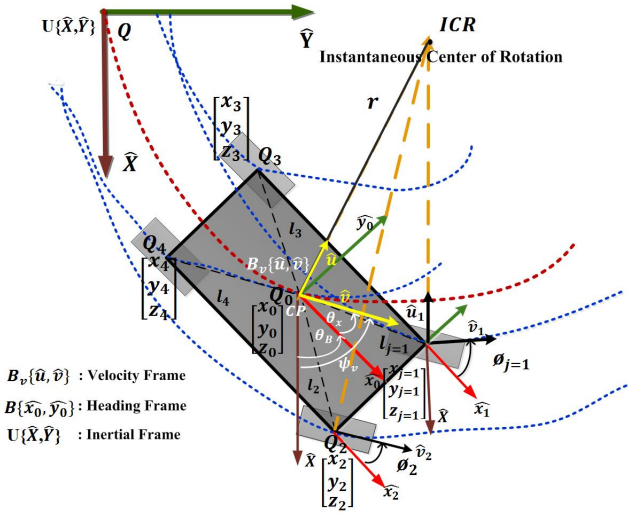

Fig. 4. Using the generated synchronized trajectories and corresponding traces for the robot and wheels center points belonging to each single robot, we easily obtain the robot kinematic variables. Then, to plan the robot velocity, we estimate the ICR point which is defined as the intersection points of wheels axis.

written as $[cos(\phi_j)\ sin(\phi_j)\ 0]$ and $v_j\hat{\mathbf{v}}_j$ is the velocity vector of the Q_j obtained from the generated trajectories. After obtaining the necessary kinematic variables, we put them in the the following kinematic constraint which describes the relationship between velocity in Q_0 and the legs velocities in Q_j:

$$^{\mathbf{B}}\hat{\mathbf{v}} = \mathbf{R}(\psi_v - \theta_B)[1,0,0]^T, \tag{7}$$

$$v_j^{\mathbf{B}}\hat{\mathbf{v}}_\mathbf{j} = v^{\mathbf{B}}\hat{\mathbf{v}} + \omega_B(\hat{\mathbf{z}} \times^{\mathbf{B}} \hat{\ell}_\mathbf{j}), \tag{8}$$

where $\mathbf{R}(\psi_v - \theta_B)$ is the rotation matrix with angle $(\psi_v - \theta_B)$ around the $z-$axis and $\hat{\mathbf{z}} = [001]^T$.

Unsynchronized wheels of mobile robots results in slippage and misalignment in translation and rotation movement as well as several other issues, discussed in [20]. To overcome these problems, the points on the generated trajectories for all wheels in a conventional trajectory planning method have to form a unique intersection point of all wheels axis [21]. To plan the robots linear and angular velocities, it is necessary to obtain a unique instantaneous center of rotation (ICR) at each trajectory point belonging to the robot body. In our proposed method, by knowing the synchronized trajectories for each wheel, we can easily obtain the ICR, which is on the horizontal Cartesian plane with zero velocity, while undergoing planar movement [22]. Based on the ICR that illustrated in Figure 4, the relationship between ω_B and v_B in the frame $\mathbf{B}$ is:

$$\omega_B = \frac{v_B}{r}, \tag{9}$$

where r is the distance between the robot's ICR and Q_0. v_B and ω_B are the liner and angular velocities of Q_0 respectively. Therefore, substituting r in (8) gives the relation between the velocity of robot-CP and the velocity of its four wheels:

$$v_j = v_B \|(\hat{\mathbf{v}} + \frac{1}{r}(\hat{\mathbf{z}} \times \overrightarrow{\ell_\mathbf{j}})\| \tag{10}$$

The curvature κ_j gives the relation between the driving velocity of each wheel v_j, and its steering velocity $\dot{\phi}_j$:

$$\kappa_j = \frac{\dot{\phi}_j}{v_j}, j = 1..., 4. \tag{11}$$

Then, we find the steering velocity for each wheel:

$$\omega_j = \dot{\phi}_j = (\kappa_j.v_B)\|(\hat{\mathbf{v}} + \frac{1}{r}(\hat{\mathbf{z}} \times \overrightarrow{\ell_\mathbf{j}})\|. \tag{12}$$

The tangent in each point belonging to the generated trajectories for $\{Q_j, j = 1..., 4\}$ gives $\hat{\mathbf{v}}_\mathbf{j}$ and $\hat{\mathbf{u}}_\mathbf{j}$ simply. In addition, each wheel follows the ICR at its defined center point, such that it coincides with vector $\hat{\mathbf{u}}_\mathbf{j}$ and intersects at the ICR point.

The mobile, robot generated trajectories for all wheels are synchronized. This means that by selecting two generated paths out of four, and placing the robot-CP on them, the remaining attached points will coincide with the respectively generated paths. Thus, two v_js are sufficient to calculate the ICR position. As illustrated in Figure. 4, the distance between Q_0 and ICR point r is calculated using the following geometrical relation:

$$x_r = \frac{v_1.x_2 - v_2(x_1 + v_1(y_1 - y_2))}{v_1 - v_2},$$
$$y_r = \frac{x_1 - x_2 + v_1.y_1 - v_2.y_2}{v_1 - v_2},$$
$$r = \sqrt{(x_0 - x_r)^2 + (y_0 - y_r)^2}. \tag{13}$$

Therefore, substituting the r in (10) gives the relation between the Q_0 and its wheels steering and driving velocities. The necessary kinematic variables via vision-based generated trajectories are then ready to plan the steering and driving velocities for the robot-CP and four wheels' center points.

IV. BOUNDED VELOCITY PLANNING

In this section, we define the strategy to plan the maximum allowable bounded velocity for each single mobile robot with 4WS. Our desired mobile robot has the maximum driving velocity V_{max}^D, and the maximum steering velocity $\dot{\phi}_{max}^S$. As explained above, at each point belonging to the trajectory, the curvature can estimated easily. The relation between the velocity of the center of mobile robot v_B and the velocity of each wheel's v_j is defined via (10). Therefore, a mobile robot with four independently steered wheels has eight velocity candidates to fulfill four driving and steering constraints.

Thus, at each point of the generated trajectory, only one of the driving or steering velocities of each wheel may have the maximum value. Therefore, for each wheel $\{Q_j, j = 1, 2, 3, 4\}$, first we evaluate $V_{j,max}$, that is the maximum driving velocity of the wheel j that keeps its driving and steering velocities bounded [5]:

$$V_{j,max} = min(V_{max}^D, \frac{\dot{\phi}_{max}^S}{\mid \kappa_j \mid}) \tag{14}$$

Then, we evaluate $v_{B,j}$, which is a candidate for the base velocity v_B, and is divided based on the maximum driving velocities of the j wheel [5]:

$$v_{B,j} = \frac{V_{j,max}}{\|((\hat{\mathbf{v}} + \frac{1}{r}(\hat{\mathbf{z}} \times \overrightarrow{\ell_{\mathbf{j}}})\|} \tag{15}$$

Now we evaluate the velocity of robot-CP v_B:

$$v_B = min(v_{B,j}), j \in 1, 2, 3, 4. \tag{16}$$

Based on (14), if κ_j becomes small enough, ($V^S_{j,max} = \dot{\phi}^S_{j,max}$) will exceed V^D_{max}, therefore the driving velocity should be bounded by V^D_{max}. In addition, if the curvature increases, $V^S_{j,max}$ decreases and the steering velocity becomes critical. In this case, the driving velocity should not exceed $V^S_{j,max}$ thus, that steering velocity stays below $\dot{\phi}^S_{max}$.

V. PATH COORDINATION FOR MULTIPLE MOBILE ROBOTS WITH 4WS

The path coordination for multiple mobile robots along generated paths is a classical problem that addresses how multiple mobile robots move to reach their goals in the shared workspace while avoiding mutual collisions as well as static obstacles. Let us consider n mobile robots with four steering wheels that start to move in the shared workspace on horizontal plane, simultaneously. The calibrated camera mounted over the workspace has a limited field of view. Therefore, depending on the geometrical size of the robots' platforms, limited number of mobile robots can move in the shared workspace. In this paper, we propose a decoupled and prioritized path planning approach in the shared configuration time-space for multiple mobile robots with 4WS.

A. Paths and Traces

As described in Section II, we proposed a method to plan obstacle-free paths for each robot in a shared workspace without taking in to account the paths of the other robots. Nonholonomic mobile robots with 4WS can move in any direction without changing the heading angle. Therefore, generating the corresponding paths is more difficult than conventional holonomic mobile robots. The synchronized generated paths determine the whole volume swept by each mobile robot where the heading angle is already computed for each generated midpoint. The domain swept by each mobile robot when moving along the path is called a trace [14]. Here, by utilizing the generated synchronized paths, the geometrical traces can be obtained as the square shape of a mobile robot plus the space swept by its wheels in the world coordinates with respect to the inertial frame.

B. Trajectory Coordination

Trajectory coordination determines the robots position and velocity along a given generated path while avoiding stationary obstacles as well as mutual collision. To coordinate the motion of multiple mobile robots along their generated obstacle-free paths, it is necessary to compute the intersection region that can be achieved using individual traces that may intersect in the shared configuration time-space [12]. The geometrical traces that explained above determine not only the intersection region between the multiple mobile robots but also the edges of the mobile robot wheels that may intersect with another moving mobile robot, in time-space configuration. Therefore we are able to estimate the time of collision with desired velocities in the generated paths. As explained before, by utilizing the proposed vision-based method, planning maximum bounded steering and driving velocities are simplified considerably.

C. Prioritization

Based on the basic concept of prioritization in a shared workspace, collision between multiple robots is resolved by introducing a priority scheme. Consider multiple mobile robots start to move simultaneously and the mobile robot with highest priority must first move to avoid only the static obstacle. The mobile robots with lower priority move in its generated path to avoid both the stationary and highest priority mobile robots. The lower priority mobile robots switch to the halt mode in their intersection boundaries and waits for the higher priority mobile robots to pass and continue the process to reach their desired goals.

Here, the generated geometrical traces for robots that move forward in time-space are employed to assign the priorities of the moving mobile robots in sequence. We assume multiple mobile robots start to move simultaneously with maximum allowable velocities. The generated geometrical trajectories determine the possibility of mutual collision in the whole shared workspace may occur.

Due to the limited number of mobile robots in such a confined workspace, we have to consider all possible assignments. Based on the generated trajectories that determine the possible intersection regions, the mobile robot that must move to avoid only the static obstacles has higher priority. Furthermore, the mobile robot that must move to avoid both the stationary and higher priority mobile robot has lower priority. The lower priority mobile robots switch to the halt mode to avoid the intersection boundaries and wait for the higher priority mobile robots to pass. The generated trajectories and corresponding traces with respect to the robot inertial-frame in time-space configuration determine the minimum time of the halting mode for lower priority mobile robots. Time delays are inserted to resolve potential collisions. This process is continued until all of the mobile robots with 4WS reach their individual goals.

VI. EXPERIMENTAL RESULTS

In this section, we show the effectiveness of the proposed vision-based path coordination method for multiple mobile robots with 4WS, using a fixed overhead camera. The CCD calibrated camera mounted over the workspace has a limited field of view. Thus, depending on the geometrical size of the robots' platforms limited number of mobile robot can move in the shared workspace. Table I lists the specifications and limits of the wheels' actuator velocities of mobile robot with 4WS [5].

Each mobile robot comprised of a rigid base and four steering wheels, each of which equipped with two independent servo drives with two DOF in a horizontal motion plane. The simple 3D CAD model of the mobile robot is designed so that robot-CP coincides with its CAD center-gravity and wheels-CP coincide with its wheels vertical axis mapped in the ground (Fig. 3). In each experiment we randomly chose the starting and target locations of the robots.

TABLE I

SPECIFICATIONS OF NONHOLONOMIC MOBILE ROBOT WITH 4WS

Description	Quantity
Distance Between Two Wheels (x direction)	655 mm
Distance Between Two Wheels (y direction)	335 mm
Maximum Velocity of Steering Wheel Actuator	$1^{rad}/_{sec}$
Maximum Velocity of Driving Wheel Actuator	$600^{mm}/_{sec}$

In experiment 1, the goal is vision-based path coordination for two mobile robots with 4WS and the same characteristic, to move with maximum allowable velocities. As explained before, due to the limited number of mobile robots in such a confined workspace, we first consider all possible priorities for all robots in intersection boundaries. Then, by utilizing the generated trajectories and its corresponding traces in time-workspace, we determine the priorities to all mobile robots.

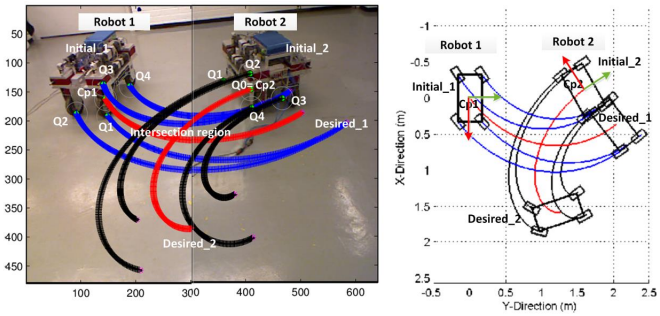

Fig. 5. Experiment 1: First, we plan individual paths for both mobile robots in the image space to only avoid them from image boundaries (left). The generated paths gives their corresponding traces in the world coordinates with respect to the inertial-frame in CP1 (right).

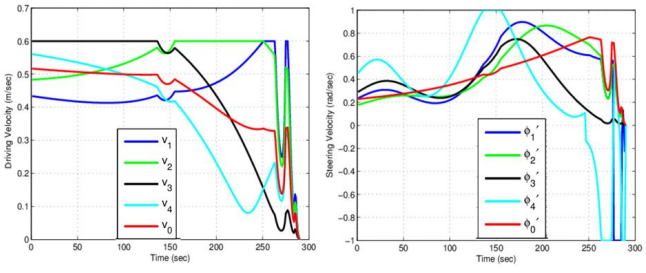

Fig. 6. Experiment 1: Generated synchronized trajectories for Robot-1, gives the kinematic variables to obtain the maximum allowable driving velocities (left), and maximum allowable steering velocities (right), for Robot-1's body and wheels, without considering the possible mutual collision.

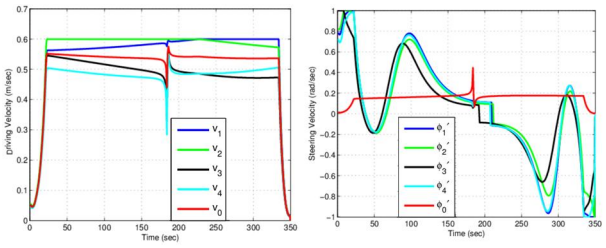

Fig. 7. Experiment 1: Planned maximum allowable driving velocities (left), and maximum allowable steering velocities (right), for Robot-2's body and wheels, without considering the possible mutual collision.

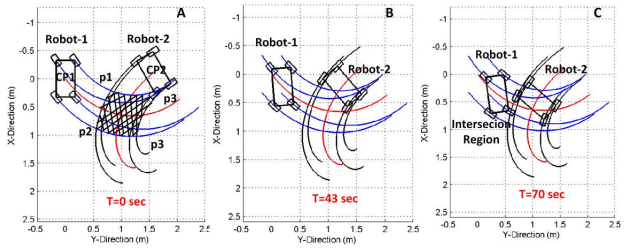

Fig. 8. Experiment 1: By utilizing the geometrical traces, we determine that Robot-2 has a higher priority than Robot-1, A. Two sequences of mutual collision without considering a priority are shown in B and C.

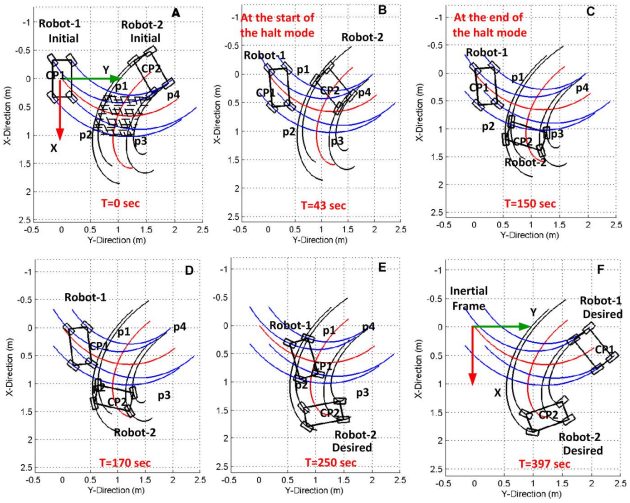

Fig. 9. Experiment 1: In T=0 sec, hatched region which is pointed with $p1$-$p4$ determines the intersection boundaries between Robot-1 and Robot-2 in the world coordinates, A. Robot-2 has higher priority than Robot-1, B. The lower priority robot must switch to the halt mode in T=43 sec till T=150 sec to pass the Robot-2 with higher priority, B and C. The traces of Robot-1 and Robot-2 in T=170 sec are shown in D. In T=250 sec when Robot-2 almost reaches its goal is shown in E. Robot-1 reaches its goal in T=397 sec, F.

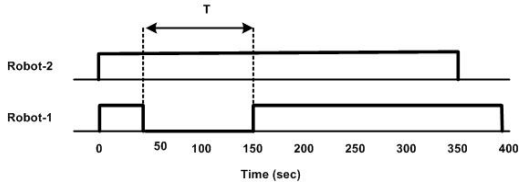

Fig. 10. Experiment 1: The lower priority Robot-1 with maximum allowable velocities switches to the halt mode in T=43 and waits 107 sec, until Robot-2 with higher priority and maximum allowable velocities passes the intersection region.

In experiment 2, the goal is path coordination for three mobile robots with 4WS in shared confined workspace to move with maximum allowable velocities and reach their individual goals. The mobile robots must move without mutual collision and avoid both static obstacle and image boundaries.

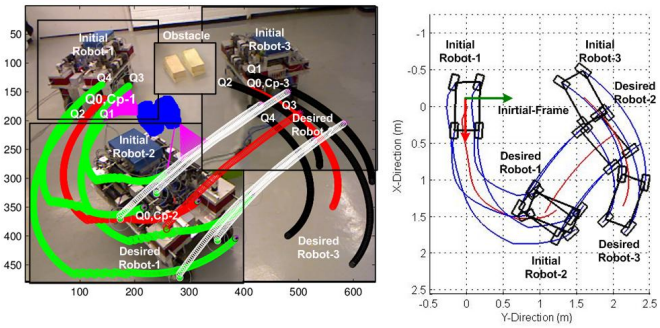

Fig. 11. Experiment 2: Generated individual paths are illustrated for three mobile robots in the image space while avoiding two types of obstacles including: (1) recognized static obstacles in the image space (two bricks) and (2) image boundaries (left). Figure shows their corresponding traces in the world coordinates and with respect to the inertial-frame in CP-1 (right).

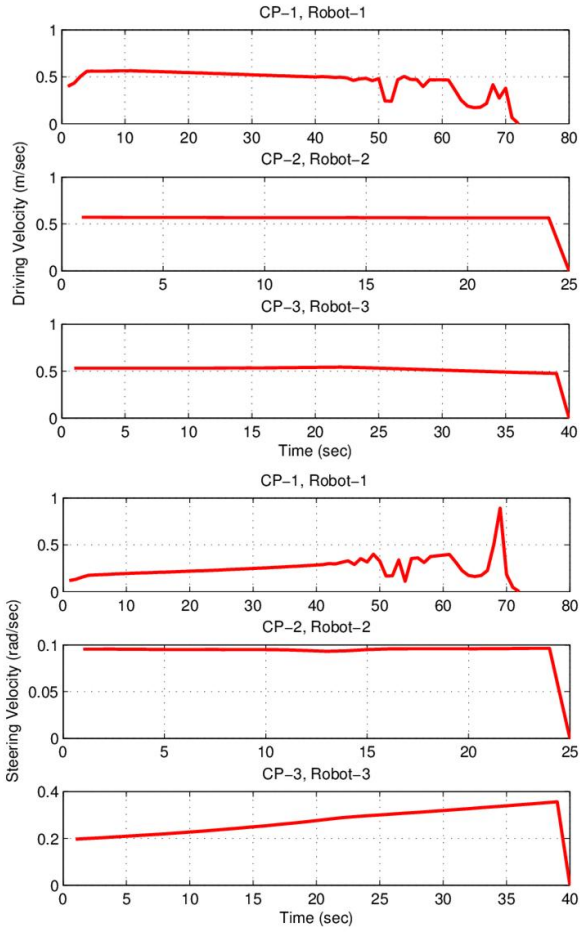

Fig. 12. Experiment 2: Planned maximum allowable driving velocities (up), and steering velocities (down) independent of the other mobile robots for center-points of Robot-1, Robot-2 and Robot-3 respectively.

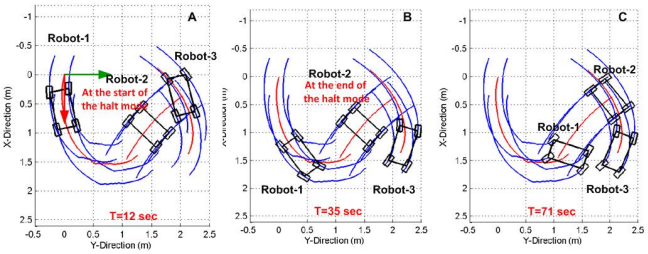

Fig. 13. Experiment 2: By utilizing the generated traces for three mobile robots, we determine how to assign the priorities for mobile robots in the shared workspace, A. Robot-2 has lower priority than Robot-3 and also Robot-1. Robot-2 must switch to the halt mode in T=12 sec for 23 sec, to pass Robot-3 without mutual collision, A, B. Three mobile robots reach their goals in T=71 sec, D.

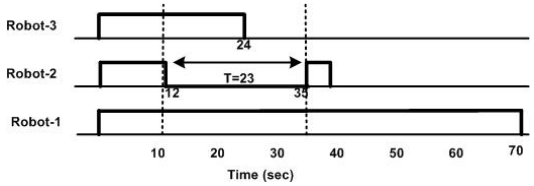

Fig. 14. Experiment 2: The lowest priority Robot-2 with maximum allowable velocity switches to the halt mode and waits for T= 23 sec until Robot-3 with highest priority passes the intersection region.

VII. CONCLUSION

This paper presents the decoupled vision-based path coordination method for nonholonomic omnidirectional mobile robots with four steering wheels in a shared and confined workspace using only one overhead camera. We have developed the vision-based path planning method to generate the synchronized obstacle-free trajectories for robot's wheels and robot's center-point, simultaneously. These synchronized trajectories simplify the complexity of the kinematic model for such mobile robots to easily estimate the necessary variables of kinematic models. Then we plan maximum allowable driving and steering velocities.

The proposed path coordination method determines the intersection region, computed using generated synchronized trajectories in the time-space configuration. Due to the limited number of mobile robots in such a confined workspace, by utilizing the generated traces, we determine the priorities for each mobile robot. We can compute the minimum time delay for lower priority mobile robot to avoid mutual collision in the intersection region. The driving and steering velocity profiles for higher and lower priority mobile robots, taking into account a delay time are computed to plan the new velocities profile for all mobile robots.

REFERENCES

[1] J. P. Trevelyan, S.-C. Kang, and W. R. Hamel, "Robotics in hazardous applications," in *Springer Handbook of Robotics*. Springer, 2008, pp. 1101–1126.

[2] L. E. Parker, "Path planning and motion coordination in multiple mobile robot teams," *Encyclopedia of Complexity and System Science. Springer, Heidelberg*, 2009.

[3] S. Liu, D. Sun, and C. Zhu, "Coordinated motion planning for multiple mobile robots along designed paths with formation requirement," *Mechatronics, IEEE/ASME Transactions on*, vol. 16, no. 6, pp. 1021–1031, 2011.

[4] R. Oftadeh, R. Ghabcheloo, and J. Mattila, "A novel time optimal path following controller with bounded velocities for mobile robots with independently steerable wheels," in *Intelligent Robots and Systems (IROS), 2013 IEEE/RSJ International Conference on*. IEEE, 2013, pp. 4845–4851.

[5] R. Oftadeh, M. M. Aref, R. Ghabcheloo, and J. Mattila, "Bounded-velocity motion control of four wheel steered mobile robots," in *Advanced Intelligent Mechatronics (AIM), 2013 IEEE/ASME International Conference on*. IEEE, 2013, pp. 255–260.

[6] R. S. Rao, V. Kumar, and C. J. Taylor, "Planning and control of mobile robots in image space from overhead cameras," in *Robotics and Automation, 2005. ICRA 2005. Proceedings of the 2005 IEEE International Conference on*. IEEE, 2005, pp. 2185–2190.

[7] V. J. Lumelsky and K. Harinarayan, "Decentralized motion planning for multiple mobile robots: The cocktail party model," in *Robot colonies*. Springer, 1997, pp. 121–135.

[8] G. Wagner and H. Choset, "M*: A complete multirobot path planning algorithm with performance bounds," in *Intelligent Robots and Systems (IROS), 2011 IEEE/RSJ International Conference on*. IEEE, 2011, pp. 3260–3267.

[9] P. Abichandani, H. Y. Benson, and M. Kam, "Decentralized multi-vehicle path coordination under communication constraints," in *Intelligent Robots and Systems (IROS), 2011 IEEE/RSJ International Conference on*. IEEE, 2011, pp. 2306–2313.

[10] C. Chen, H. Qin, and Z. Yin, "Trajectory planning for omni-directional mobile robot based on bezier curve, trigonometric function and polynomial," in *Intelligent Robotics and Applications*. Springer, 2012, pp. 352–364.

[11] E.-j. Jung, B.-J. Yi, and W. K. Kim, "Motion planning algorithms of an omni-directional mobile robot with active caster wheels," *Intelligent Service Robotics*, vol. 4, no. 3, pp. 167–180, 2011.

[12] T. Siméon, S. Leroy, and J.-P. Lauumond, "Path coordination for multiple mobile robots: A resolution-complete algorithm," *Robotics and Automation, IEEE Transactions on*, vol. 18, no. 1, pp. 42–49, 2002.

[13] A. Samani, A. Abdollahi, H. Ostadi, and S. Z. Rad, "Design and development of a comprehensive omni directional soccer player robot," *International Journal of Advanced Robotic Systems*, vol. 1, no. 3, pp. 191–200, 2004.

[14] T. Simeon, S. Leroy, and J.-P. Laumond, "A collision checker for car-like robots coordination," in *Robotics and Automation, 1998. Proceedings. 1998 IEEE International Conference on*, vol. 1. IEEE, 1998, pp. 46–51.

[15] Z. Ziaei, R. Oftadeh, and J. Mattila, "Global path planning with obstacle avoidance for omnidirectional mobile robot using overhead camera," in *Mechatronics and Automation (ICMA), 2014 IEEE International Conference on*. IEEE, 2014, pp. 697–704.

[16] M. Ulrich, C. Wiedemann, and C. Steger, "Cad-based recognition of 3d objects in monocular images," in *International Conference on Robotics and Automation*, vol. 1191, 2009, p. 1198.

[17] http://www.halcon.com/halcon/.

[18] C. W. Warren, "Global path planning using artificial potential fields," in *Robotics and Automation, 1989. Proceedings., 1989 IEEE International Conference on*. IEEE, 1989, pp. 316–321.

[19] M. G. Park and M. C. Lee, "A new technique to escape local minimum in artificial potential field based path planning," *KSME international journal*, vol. 17, no. 12, pp. 1876–1885, 2003.

[20] U. Schwesinger, C. Pradalier, and R. Siegwart, "A novel approach for steering wheel synchronization with velocity/acceleration limits and mechanical constraints," in *Intelligent Robots and Systems (IROS), 2012 IEEE/RSJ International Conference on*. IEEE, 2012, pp. 5360–5366.

[21] D. Wang and F. Qi, "Trajectory planning for a four-wheel-steering vehicle," in *Robotics and Automation, 2001. Proceedings. ICRA'01. IEEE International Conference on*. IEEE, 2001.

[22] C. P. Connette, A. Pott, M. Hagele, and A. Verl, "Control of an pseudo-omnidirectional, non-holonomic, mobile robot based on an icm representation in spherical coordinates," in *Decision and Control, 2008. CDC 2008. 47th IEEE Conference on*. IEEE, 2008, pp. 4976–4983.